$CH_2CHOH_2^+$ + PN: A Proton-Transfer Triple Play[1]

Simon Petrie*

Department of Chemistry, the Faculties, Australian National University, Canberra ACT 0200, Australia

Received: February 11, 2005; In Final Form: April 14, 2005

Quantum chemical calculations are used to explore the proton-transfer reactivity of O-protonated vinyl alcohol, $CH_2CHOH_2^+$, with phosphorus nitride, PN. This reaction is relevant to the chemical evolution of interstellar clouds, since O-protonated vinyl alcohol has been postulated (and tentatively identified) as a product of the association reaction between interstellar H_3O^+ and C_2H_2, while PN is the most widespread and abundant phosphorus-containing molecule seen in astrophysical environments. Furthermore, the reaction exhibits an unusual mechanistic feature, namely, an extended "proton-transport catalysis" mechanism, which we characterize here as a "proton-transfer triple play". The reaction proceeds initially by proton transfer from $CH_2CH\boldsymbol{O}H_2^+$ to P***N***, then from P***N***H^+ to $\boldsymbol{C}H_2CHOH$, and finally from $CH_3CH\boldsymbol{O}H^+$ to P***N***, where the emphasized atom indicates the resultant site of protonation/deprotonation. Thus, the ultimate overall bimolecular proton-transfer reaction is expected to occur as $CH_2CHOH_2^+ + PN \rightarrow CH_3CHO + PNH^+$; that is, the apparent favored product channel exhibits not only proton transfer but also keto/enol tautomerization. The triple-play mechanism can be rationalized in terms of the proton affinities of vinyl alcohol, acetaldehyde, and phosphorus nitride, which here are satisfactorily reproduced by high-level ab initio calculations. Other neutrals with a proton affinity appropriate for the possible triple-play mechanism converting $CH_2CHOH_2^+$ to CH_3CHO are also identified, with a view to encouraging experimental investigation of this mechanism.

1. Introduction

Protons are fickle creatures, flitting effortlessly from site to site in a manner which may well be the envy of other, larger, heavier functional groups. It is commonplace, within gas-phase ion/molecule reactions, for a proton-transfer channel which may only be exothermic by, say, 2 kJ mol^{-1} to compete effectively against other channels whose exothermicities may well be several hundred kilojoules per mole. This tendency for proton transfer to be almost invariably efficient when exothermic has greatly aided our understanding of the thermochemistry of proton-bearing ions. One of the key thermochemical properties of such ions, the proton affinity (PA),[2,3] defined as the exothermicity of protonation

$$H^+ + X \rightarrow XH^+ \qquad PA(X) = -\Delta H^\circ_{react} = \Delta H^\circ_f(H^+) + \Delta H^\circ_f(X) - \Delta H^\circ_f(XH^+) \quad (1)$$

provides a direct indication for the tendency of proton transfer to occur from a reactant ion XH^+ to a neutral Y. Proton transfer is exothermic, and almost always highly efficient,[4] if PA(X) < PA(Y).

Proton transfer can also offer a route to tautomerization. If two isomeric ions HAB^+ and ABH^+ have different formation enthalpies, it follows that the proton affinity of AB at site A differs from that of AB at site B. For example, PA(C***O***) = 426.3 kJ mol^{-1}, whereas PA(***C***O) = 594.0 kJ mol^{-1},[3] reflecting the preference for carbon monoxide protonation to occur at atom C. In isolation, COH^+ and HCO^+ both enjoy substantial kinetic stability due to the very high interconversion barrier between these isomers,[5] but if the higher-energy isomer COH^+ encounters a species X for which 426.3 < PA(X) < 594.0 kJ mol^{-1}, the most exothermic proton-transfer outcome is the product channel $HCO^+ + X$,[6] which arises by a mechanism termed "proton-transport catalysis":[7]

$$COH^+ + X \rightarrow [COH^+\cdots X] \rightarrow [CO\cdots{}^+HX] \rightarrow [OC\cdots{}^+HX] \rightarrow [OCH^+\cdots X] \rightarrow OCH^+ (HCO^+) + X \quad (2)$$

Direct identification of such a proton-transport catalysis product channel is frustrated, in mass-spectrometric studies, by the identical *m*/*z* ratio of reactant and product ions, and this author recollects several perplexing months of Ph.D. research in which both student and supervisors were mystefied by the unexpected reluctance of HCN^+ to exhibit proton transfer to either CO or CO_2, contrary to the established proton affinities of the species involved. The subsequent identification of $HNC^+ + CO$ (or CO_2) as the ultimate, most exothermic, bimolecular product channel of the $HCN^+ + CO$ (or CO_2) reaction was effected using a "monitor gas" (CF_4 or SF_6) which reacted in a measurably different manner with HCN^+ than with HNC^+.[8] Many experiments have now established the occurrence of proton-transport catalysis in various reactions of $NNOH^+$ (more stable isomer, $HNNO^+$),[9,10] COH^+ (HCO^+),[6] HCN^+ (HNC^+),[8] $HSiO^+$ ($SiOH^+$),[11] $CF_3OH_2^+$ ($HFCF_2OH^+$),[12] CH_3OH^+ ($CH_2OH_2^+$),[13] CH_3CHO^+ (CH_2CHOH^+),[14] $CH_3C(O)NH_2^+$ ($CH_2C(OH)NH_3^+$),[15] $H_2O{\cdot}CO^+$ ($HOCOH^+$),[16] and $HCOH^+$ (CH_2O^+)[17] among others.

The prototypical proton-transport catalysis system, involving the COH^+/HCO^+ isomer pair, is highly pertinent to the gas-phase chemistry of interstellar clouds.[6,18−20] Isomerism of neutral and protonated C_2H_4O also holds deep interstellar relevance. Acetaldehyde, vinyl alcohol, and ethylene oxide constitute the first set of isomeric "triplets" to have been identified in interstellar clouds,[21,22] while there has been debate concerning the identity of the $C_2H_5O^+$ product of the $H_3O^+ + C_2H_2$

* E-mail: simon.petrie@anu.edu.au.

10.1021/jp0507389 CCC: $30.25
Published on Web 06/22/2005

association reaction proposed as a route to one or more of the interstellar C_2H_4O isomers.[23,24] An experimental selected-ion flow tube (SIFT) study of the $H_3O^+ + C_2H_2$ association reaction has established that it produces two distinct $C_2H_5O^+$ isomers of differing reactivity, which are thought to be $CH_2CHOH_2^+$ and either $H_3O^+ \cdot C_2H_2$ or CH_3CHOH^+.[24] Other experimental investigations have established that CH_3CHOH^+ is the lowest in energy of several distinct isomers,[25−28] while several theoretical studies[24,29−35] have found that, while the barrier separating $H_3O^+ \cdot C_2H_2$ and $CH_2CHOH_2^+$ is comparatively modest and is submerged relative to $H_3O^+ + C_2H_2$, a considerably higher barrier inhibits interconversion of $CH_2CHOH_2^+$ and CH_3CHOH^+. The latter barrier, which at the Gaussian-2 (G2) level of theory lies 173 kJ mol^{-1} above the total energy of the higher-energy ($CH_2CHOH_2^+$) isomer,[24] protrudes 31 kJ mol^{-1} above the total energy of the reactants $H_3O^+ + C_2H_2$, thereby apparently precluding formation of the global minimum CH_3CHOH^+ in this association reaction at low temperature. The study of Fairley et al.[24] also reported calculated values for the "O-protonation" proton affinities of CH_3CHO (770.0 kJ mol^{-1}) and CH_2CHOH (721.7 kJ mol^{-1}) which are in good agreement with existing experimental results.

In the present work, high-level ab initio methods are used to characterize stationary points on the $[C_2H_5O/PN]^+$ potential energy surface, with the aim of illuminating the proton-transfer chemistry of $CH_2CHOH_2^+$ with PN. Phosphorus nitride was chosen for this theoretical study because (a) it is a known interstellar molecule,[36,37] and therefore a plausible reactant with $CH_2CHOH_2^+$ in the environments thought to contain this ion; (b) it is not a laboratory-stable species, and thus theory offers an excellent means of obtaining reactivity information not otherwise accessible; and (c) it has a proton affinity between those of CH_3CHO at O (768.5 kJ mol^{-1}) and CH_2CHOH at C (811.2 kJ mol^{-1}), which we identify here as the crucial PA range for "triple-play" proton transfer from $CH_2CHOH_2^+$.

2. Theoretical Methods

Quantum chemical methods are applicable across an extremely wide range of chemical problems. In the context of protonation thermochemistry, high-level quantum chemical approaches are routinely able to predict or determine the proton affinities of small molecules to an accuracy matching the most precise experimental measurements.[38−40]

In the present work, calculations variously employ the CBS-QB3[41,42] and CBS-APNO[43] "model chemistry" approaches as well as the CCSD(T)/AUG-cc-pVTZ level of theory. The "complete basis set" (CBS) methods use calculations at various levels of theory and attempt extrapolation to the basis set limit, that is, to the hypothetical infinite set of mathematical basis functions which perfectly describes the molecular wave function of interest. Of the two CBS methods used here, CBS-QB3[44] is a less computationally intensive method which uses a generally grosser (but nevertheless acceptable) set of approximations and assumptions, while CBS-APNO ("atomic pair natural orbital")[43] is more rigorous and more computationally demanding. A limitation of CBS-APNO is its applicability only to species comprised entirely of first-row atoms (therefore precluding calculations on PN), while CBS-QB3 is applicable to all main-group elements up to Kr.

The other high-level approach used here, CCSD(T)/AUG-cc-pVTZ, uses the coupled-cluster treatment of electron correlation including single, double, and perturbative triple excitations[47,48] in conjunction with the AUGmented, correlation consistent, polarized valence-triple-zeta basis sets of Dunning and co-workers.[49−51] For these calculations, optimized geometries and zero-point vibrational energies of the requisite stationary points were first obtained in B3-LYP/AUG-cc-pVTZ optimization and frequency calculations.

All calculations were performed using the Gaussian 98 program suite.[52]

3. Results and Discussion

3.1. Proton Affinities of C_2H_4O Isomers. The principal features of the $C_2H_5O^+$ potential energy surface (PES) appear well established as a result of the many experimental[24−28] and theoretical[24,29−35] studies which have focused on this system. Our CBS-QB3, CBS-APNO, and CCSD(T)/AUG-cc-pVTZ calculations on the proton affinities of various C_2H_4O isomers, shown in Table 1, are all in good agreement with the literature values.

Within the computed proton affinity values, several trends are evident. The CBS-QB3 values are uniformly lower than the literature values, with a discrepancy exceeding 5 kJ mol^{-1} only in the case of *c*-C_2H_4O, for which we obtain a PA value 10.4 kJ mol^{-1} below the experimental result. The CBS-QB3 PA values are also consistently lower than the corresponding CBS-APNO values; the latter generally show better agreement with experiment, although for C-protonation of CH_2CHOH the CBS-APNO result exceeds the literature result by 7.2 kJ mol^{-1}, a greater disparity than what is seen between experiment and CBS-QB3 for this quantity. It should be noted, however, that the C-proton affinity of vinyl alcohol has not been measured directly: the "experimental" value which we list is an indirect determination based on PA(CH_3CHO) and the experimental difference in $\Delta H°_{f,298}$ values for CH_3CHO and CH_2CHOH. Consequently, the experimental value PA($\boldsymbol{C}H_2CHOH$) = 811.2 kJ mol^{-1} should be regarded as having a somewhat larger uncertainty than many typical constituents of the literature proton affinity ladder. For both this quantity and PA(*c*-C_2H_4O), CBS-APNO shows much better agreement with previously reported G2 calculations[24] than with experiment.

The CCSD(T)/AUG-cc-pVTZ calculations are reported here both with ("CP") and without counterpoise corrections for basis set superposition error. Inclusion of a counterpoise correction consistently lowers the calculated proton affinity by ~8 kJ mol^{-1}; it is not, however, clear whether the counterpoise correction results in an improvement in performance. In general, the uncorrected CCSD(T) calculations show very good agreement with CBS-APNO and reasonable agreement also with CBS-QB3. All four methods consistently deliver values which display "internal" agreement within 10 kJ mol^{-1}. The latter observation, coupled with the generally good agreement of all methods with experiment, is encouraging in the sense that CBS-QB3, which is by far the "cheapest" of the four methods, can nevertheless be relied upon to produce accurate results for larger systems (for example, in the present context, collision complexes of $CH_2CHOH_2^+$ with other molecules).

3.2. Proton Affinities of Sundry Other Molecules. The methods employed in section 3.1 have also been applied here to the proton affinities of other small molecules in the (literature) PA range from 775 to 810 kJ mol^{-1}; these results are summarized in Table 2. In the context of the present work, the values for PN are the most directly relevant portions of Table 2. The literature value[3] PA(PN) = 789.4 kJ mol^{-1} is based on a selected-ion flow tube (SIFT) bracketing study of the reactions of PNH^+ with PH_3 and with C_2H_5CN;[59] the PA value derived from this study has an indicated uncertainty of ±6 kJ mol^{-1}.

TABLE 1: Theoretical Proton Affinities of the Low-Energy C_2H_4O Isomers, Determined at the CBS-QB3, CBS-APNO, and CCSD(T,full)/AUG-cc-pVTZ//B3-LYP/AUG-cc-pVTZ Levels of Theory

			E_0[b]/hartrees		PA[c]/kJ mol^{-1}			
neutral, X	ion, XH^+	method[a]	X	XH^+	0 K	298 K	lit.[d]	comments
CH_2CHOH	$CH_2CHOH_2^+$	CBS-QB3	−153.565 579	−153.836 975	712.6	717.2	721.7[e]	G2 theory
CH_2CHOH	$CH_2CHOH_2^+$	CBS-APNO	−153.752 449	−154.025 859	717.8	722.4		
CH_2CHOH	$CH_2CHOH_2^+$	CCSD(T)	−153.579 155	−153.853 317	719.8	724.4		
CH_2CHOH	$CH_2CHOH_2^+$	CP-CCSD(T)	−153.579 155	−153.850 412 5	712.2	716.8		
CH_3CHO	CH_3CHOH^+	CBS-QB3	−153.582 443	−153.871 68	759.4	765.3	768.5[f]	expt
CH_3CHO	CH_3CHOH^+	CBS-APNO	−153.770 766	−154.061 967	764.5	770.2	770.0[e]	G2 theory
CH_3CHO	CH_3CHOH^+	CCSD(T)	−153.596 175	−153.888 291	767.0	772.9		
CH_3CHO	CH_3CHOH^+	CP-CCSD(T)	−153.596 175	−153.885 200	758.8	764.0		
c-C_2H_4O	*c*-$C_2H_4OH^+$	CBS-QB3	−153.539 303	−153.828 047	758.1	763.8	774.2[f]	expt
c-C_2H_4O	*c*-$C_2H_4OH^+$	CBS-APNO	−153.727 101	−154.017 460	762.3	768.0	769.1[e]	G2 theory
c-C_2H_4O	*c*-$C_2H_4OH^+$	CCSD(T)	−153.552 677	−153.845 147	767.9	773.5		
c-C_2H_4O	*c*-$C_2H_4OH^+$	CP-CCSD(T)	−153.552 677	−153.841 498	758.3	764.0		
CH_2CHOH	CH_3CHOH^+	CBS-QB3	−153.565 579	−153.871 68	803.7	808.9	811.2[g]	expt
CH_2CHOH	CH_3CHOH^+	CBS-APNO	−153.752 449	−154.061 967	812.6	818.4	820.3[h]	G2 theory
CH_2CHOH	CH_3CHOH^+	CCSD(T)	−153.579 155	−153.888 291	811.6	816.9		
CH_2CHOH	CH_3CHOH^+	CP-CCSD(T)	−153.579 155	−153.884 993	803.0	808.3		

[a] Level of theory used in calculation. "CCSD(T)" denotes calculation at the CCSD(T,full)/AUG-cc-pVTZ//B3-LYP/AUG-cc-pVTZ level. The same level of theory is used in "CP-CCSD(T)" calculations, which additionally include a counterpoise correction for basis set superposition error, calculated at the MP2(full)/AUG-cc-pVTZ level. [b] Total energy, in hartrees (1 hartree = 2625.5 kJ mol^{-1}) and including zero-point vibrational energy, of the indicated species at 0 K. [c] Calculated proton affinity at the indicated temperature. The 298 K value is obtained using also $H_{298}(H^+)$ = +0.002 36 hartrees (ref 53). [d] Literature value of the proton affinity, at 298 K unless otherwise indicated. [e] Reported by Fairley et al. (ref 24). [f] From the tabulation of Hunter and Lias (ref 3). [g] Obtained using $PA_{298}(CH_3CHO)$ from the Hunter & Lias tabulation (ref 3) combined with the difference in reported $\Delta H°_{f,298}$ values for CH_3CHO and H_2CCHOH ($\Delta H°_{f,298}(H_2CCHOH)$ = −128.0 kJ mol^{-1}, $\Delta H°_{f,298}(CH_3CHO)$ = −170.7 kJ mol^{-1} (ref 54)). [h] Obtained using the G2 theoretical value $PA_{298}(CH_3CHO)$ from Fairley et al. (ref 24) combined with the difference in reported G2 total energies for CH_3CHO and H_2CCHOH (ref 24).

TABLE 2: Theoretical Proton Affinities of Some Representative Small Molecules for Which the Literature PA Values Lie between 775 and 810 kJ mol^{-1} (the Calculated Values Have Been Determined at the CBS-QB3, CBS-APNO, and CCSD(T,full)/AUG-cc-pVTZ//B3-LYP/AUG-cc-pVTZ Levels of Theory)

			E_0[b]/hartrees		PA[c]/kJ mol^{-1}			
neutral, X	ion, XH^+	method[a]	X	XH^+	0 K	298 K	lit.[d]	comments
SiO	$SiOH^+$	CBS-QB3	−364.223 594	−364.526785	796.0	800.6	777.8[e], 792.0[f]	expt
SiO	$SiOH^+$	CCSD(T)	−364.274 845	−364.580845	803.4	807.6	814 (0 K)[g]	CEPA-1 theory
SiO	$SiOH^+$	CP-CCSD(T)	−364.274 845	−364.575757	790.0	794.2	799.6[h], 792.0 (0 K)[i]	theory
CH_3CN	CH_3CNH^+	CBS-QB3	−132.526 620	−132.822 285	776.3	781.6	779.2[e]	expt
CH_3CN	CH_3CNH^+	CBS-APNO	−132.706 490	−133.002 767	777.9	783.4	780.1[j]	G2 theory
CH_3CN	CH_3CNH^+	CCSD(T)	−132.545 230	−132.842 841	781.4	786.7		
CH_3CN	CH_3CNH^+	CP-CCSD(T)	−132.545 230	−132.839 563	772.8	778.1		
PH_3	PH_4^+	CBS-QB3	−342.680 016	−342.976 822	779.3	785.2	785.0[e]	expt
PH_3	PH_4^+	CCSD(T)	−342.721 359	−343.017 821	778.4	784.3	784.8[j]	G2 theory
PH_3	PH_4^+	CP-CCSD(T)	−342.721 359	−343.013 879	768.0	774.0		
PN	PNH^+	CBS-QB3	−395.567 995	−395.870 096	793.2	798.8	789.4[e]	expt
PN	PNH^+	CCSD(T)	−395.608 202	−395.911 930	797.4	803.0		
PN	PNH^+	CP-CCSD(T)	−395.608 202	−395.906 273	782.5	788.1		
CS	HCS^+	CBS-QB3	−435.713 895	−436.014 277	788.7	794.5	791.5[e]	expt
CS	HCS^+	CCSD(T)	−435.745 006	−436.049 174	798.6	804.4	795.6[j]	G2 theory
CS	HCS^+	CP-CCSD(T)	−435.745 006	−436.043 708	784.2	790.0		
CH_3OCH_3	$(CH_3)_2OH^+$	CBS-QB3	−154.752 199	−155.049 259	779.9	784.9	792.0[e]	expt
CH_3OCH_3	$(CH_3)_2OH^+$	CBS-APNO	−154.940 892	−155.239 909	785.1	789.8	792.0[h]	G2 theory
H_2NCN	H_2NCNH^+	CBS-QB3	−148.565 273	−148.870 630	801.7	807.4	805.6[e]	expt
H_2NCN	H_2NCNH^+	CBS-APNO	−148.751 105	−149.056 964	803.0	807.5		
H_2NCN	H_2NCNH^+	CCSD(T)	−148.579 970	−148.887 225	806.7	812.4		
H_2NCN	H_2NCNH^+	CP-CCSD(T)	−148.579 970	−148.883 961	798.1	803.8		

[a] Level of theory used in calculation. "CCSD(T)" denotes calculation at the CCSD(T,full)/AUG-cc-pVTZ//B3-LYP/AUG-cc-pVTZ level. The same level of theory is used in "CP-CCSD(T)" calculations, which additionally include a counterpoise correction for basis set superposition error, calculated at the MP2(full)/AUG-cc-pVTZ level. [b] Total energy, in hartrees (1 hartree = 2625.5 kJ mol^{-1}) and including zero-point vibrational energy, of the indicated species at 0 K. [c] Calculated proton affinity at the indicated temperature. The 298 K value is obtained using also $H_{298}(H^+)$ = +0.002 36 hartrees (ref 53). [d] Literature value of the proton affinity, at 298 K unless otherwise indicated. [e] From the tabulation of Hunter and Lias (ref 3). [f] Reported by Fox et al. (ref 55). [g] Reported by Botschwina and Rosmus (ref 56). [h] G2 theory value, reported by Lucas et al. (ref 57). [i] Average of several computed values, reported by Rodriquez et al. (ref 58). [j] Reported by Smith and Radom (ref 53).

The counterpoise-corrected CCSD(T) proton affinity agrees very well with this experimental value. The CBS-QB3 and uncorrected CCSD(T) values lie somewhat farther afield, although the CBS-QB3 value is acceptably within the 10 kJ mol^{-1} uncertainty commonly ascribed to such model chemistry methods.

Of the other species surveyed in Table 2, CH_3CN and CH_3OCH_3 have the most substantial literature records and have been repeatedly studied by both theoretical and experimental methods. The CBS-QB3, CBS-APNO, and CP-corrected CCSD(T) results for CH_3CN all tally very well with the literature value, while for CH_3OCH_3 the agreement for CBS-QB3 is poorer but still acceptably within ±10 kJ mol^{-1}. The proton affinities of SiO, PH_3, CS, and H_2NCN are perhaps less comprehensively established,[3] and for these species, there are

TABLE 3: CBS-QB3 Total Energies of Reactants, Products, and Stationary Points Implicated in the Triple-Play Proton-Transfer Process Initiated by $CH_2CHOH_2^+$ + PN

structure	ZPE[a]/mhartrees	i[b]	E_0 (0 K)[c]/hartrees	H_0 (298 K)[d]/hartrees	E_{rel} (0 K)[e]/kJ mol^{-1}	ΔH_{rel} (298 K)[e]/kJ mol^{-1}
$CH_2CHOH_2^+$ + PN	70.396	0	−549.404 970	−549.396 510	0.0	0.0
CH_2CHOH + PNH^+	70.537	0	−549.435 675	−549.427 575	−80.6	−81.6
CH_3CHOH^+ + PN	70.783	0	−549.439 675	−549.431 407	−91.1	−91.6
CH_3CHO + PNH^+	69.273	0	−549.452 539	−549.441 65	−124.9	−118.5
$CH_2CHOH{\cdot}HNP^+$ (**Ia**)	70.324	0	−549.468 138	−549.460 914	−165.8	−169.1
TS **Ia**/**Ib**	69.133	1	−549.463 351	−549.457 796	−153.3	−155.6
$CH_2CHOH{\cdot}HNP^+$ (**Ib**)	70.247	0	−549.464 335	−549.456 018	−155.9	−157.2
TS **Ib**/**Ib**	70.109	1	−549.467 251	−549.459 810	−163.5	−166.2
TS**Ib**/**IIa**	70.548	1	−549.454 741	−549.447 130	−130.7	−132.9
$PNH^+{\cdot}CH_2CHOH$ (**IIa**)	69.554	0	−549.458 117	−549.449 989	−139.5	−140.4
TS **IIa**/**IIb** ("cis")	69.156	1	−549.439 693	−549.431 864	−91.2	−92.8
TS **IIa**/**IIb** ("trans")	69.980	1	−549.450 160	−549.442 334	−118.6	−120.3
$PNH^+{\cdot}CH_2CHOH$ (**IIb**)	69.741	0	−549.456 923	−549.448 883	−134.7	−137.5
TS **IIa**/**IIIa**	67.518	1	−549.454 338	−549.446 772	−129.6	−132.0
$PN{\cdot}CH_3CHOH^+$ (**IIIa**)	71.639	0	−549.461 502	−549.453 252	−148.4	−149.0
TS **IIIa**/**IIIb**	71.495	1	−549.454 961	−549.447 146	−131.3	−132.9
$PN{\cdot}CH_3CHOH^+$ (**IIIb**)	71.571	0	−549.458 198	−549.449 359	−139.8	−138.8
TS **IIIa**/**IVa**	71.566	1	−549.459 570	−549.451 909	−143.4	−145.5
$CH_3CH(NP)OH^+$ (**IVa**)	75.041	0	−549.489 886	−549.482 930	−222.9	−226.9
TS **IVa**/**IVb** ("1")	74.104	1	−549.476 264	−549.469 842	−187.2	−192.5
TS **IVa**/**IVb** ("2")	74.250	1	−549.484 281	−549.477 852	−208.2	−213.6
$CH_3CH(NP)OH^+$ (**IVb**)	75.181	0	−549.489 220	−549.482 301	−221.2	−225.2
TS **IVa**/**Va**	72.313	1	−549.466 548	−549.459 015	−161.7	−164.1
$CH_3CHOH^+{\cdot}NP$ (**Va**)	69.708	0	−549.494 804	−549.486 777	−235.9	−237.0
TS **Va**/**Vb**	69.483	1	−549.488 875	−549.481 492	−220.3	−223.1
$CH_3CHOH^+{\cdot}NP$ (**Vb**)	69.875	0	−549.492 279	−549.484 376	−229.2	−230.7

[a] Zero-point vibrational energy in millihartrees (1 mhartree = 2.6255 kJ mol^{-1}), calculated at the B3-LYP/6-311G(2d,d,p) level of theory. [b] Number of imaginary vibrational modes in frequency calculation at the B3-LYP/6-311G(2d,d,p) level of theory. [c] Calculated total energy including zero-point vibrational energy. [d] Calculated enthalpy including zero-point vibrational energy and thermal corrections. [e] Calculated total energy (E_0), or enthalpy (H_0), at the indicated temperature, expressed relative to the reactants $CH_2CHOH_2^+$ + PN.

some discrepancies between our results and the literature values. For example, none of our computational methods can reproduce the tabulated PA(SiO) value 777.8 kJ mol^{-1}.[3] Our calculated results for SiO add to a growing body of recent experimental and theoretical determinations[55−58] which indicate that the value for this neutral, in the tabulation of Hunter and Lias,[3] is apparently too low by at least 10 kJ mol^{-1}. For PH_3, the literature record[3] shows generally good agreement between theory and experiment, with which our CBS-QB3 and uncorrected CCSD(T) results conform, although the CP-corrected CCSD(T) calculations yield a surprisingly low PA value (in almost all other instances surveyed here, the counterpoise-corrected CCSD(T) results are closer to literature values than are the uncorrected CCSD(T) values). For CS and H_2NCN, the CBS-QB3 and CP-corrected CCSD(T) values agree well with experiment, as does CBS-APNO for H_2NCN (note again that CBS-APNO is not applicable to the Si-, P-, and S-containing neutrals studied here).

The calculations detailed in Table 2 support previous studies which have suggested that proton affinity determinations using composite high-level quantum chemical approaches such as CBS-QB3 are generally reliable to within ±10 kJ mol^{-1}.[38−40] These results, coupled with those of section 3.1, indicate that CBS-QB3 is an acceptable level of theory to employ in investigation of the potential energy surface relevant to proton transfer between $CH_2CHOH_2^+$ and PN.

3.3. Stationary Points on the $[C_2H_5O/PN]^+$ Triple-Play Potential Energy Surface. Our CBS-QB3 exploration of the potential energy surface (PES) for reaction of $CH_2CHOH_2^+$ with PN reveals several isomeric proton-bound dimers as being local minima. The energetic and structural features of these species and of the transition structures (TSs) which connect them are summarized in Table 3 and Figure 1, respectively.

The energies reported in Table 3 show that no barriers between the reactants $CH_2CHOH_2^+$ + PN and the most exothermic possible proton-transfer product channel CH_3CHO + PNH^+ protrude above the energy of reactants. The absence of any entrance channel barrier is typical of gas-phase proton-transfer processes and is consistent with the expected attractive ion/dipole interaction.[60] All of the intermediate stationary points on the apparent minimum-energy pathway lie at least 125 kJ mol^{-1} below this threshold, implying that the postulated proton-transfer triple play is in principle accessible even at low temperatures. In the context of the triple play, the apparent minimum-energy pathway is seen to proceed through a sequence of five local minima (**Ib**, **IIa**, **IIIa**, **IV**, and **Va**). These minima conform, to some extent, with the expected progression through a sequence of proton-bound dimeric "collision complexes", as illustrated, for the simpler HOC^+/HCO^+ isomerization process, in reaction 2. However, it is apparent that some of the possible proton-bound dimers are not true minima: we have not been able to isolate geometries corresponding to $CH_2CHO(H)H^+{\cdot}NP$ or to $CH_3CHO{\cdot}^+HNP$. The absence of $CH_2CHO(H)H^+{\cdot}NP$ as a minimum is consistent with the considerably higher proton affinity calculated for P***N*** than for CH_2CH***O***H (see Table 1), and it is no real surprise that $CH_2CHO(H)H^+{\cdot}NP$ is unstable against the barrierless proton transfer which leads to structure **I**, $CH_2CHOH{\cdot}^+HNP$. In contrast, the absence of any minimum corresponding to $CH_3CHO{\cdot}^+HNP$ is quite counterintuitive, since the literature values and our own CBS-QB3 calculations show that CH_3CHO and PNH^+ are the lowest-energy pair of separated proton-transfer reaction products by a considerable margin (∼30 kJ mol^{-1}, according to Table 3). Evidently, the difference in proton affinity between P***N*** and CH_3CH***O*** is insufficient to retain effective N-protonation in the CH_3CHO/PN proton-bound dimer. It can be noted further that the O−H bond is markedly elongated also in both rotamers **Va** and **Vb** and also that interconversion of **Va** and **Vb** is apparently achieved not by rotation of the OH bond (and pendant PN) around the O−C axis but by proton

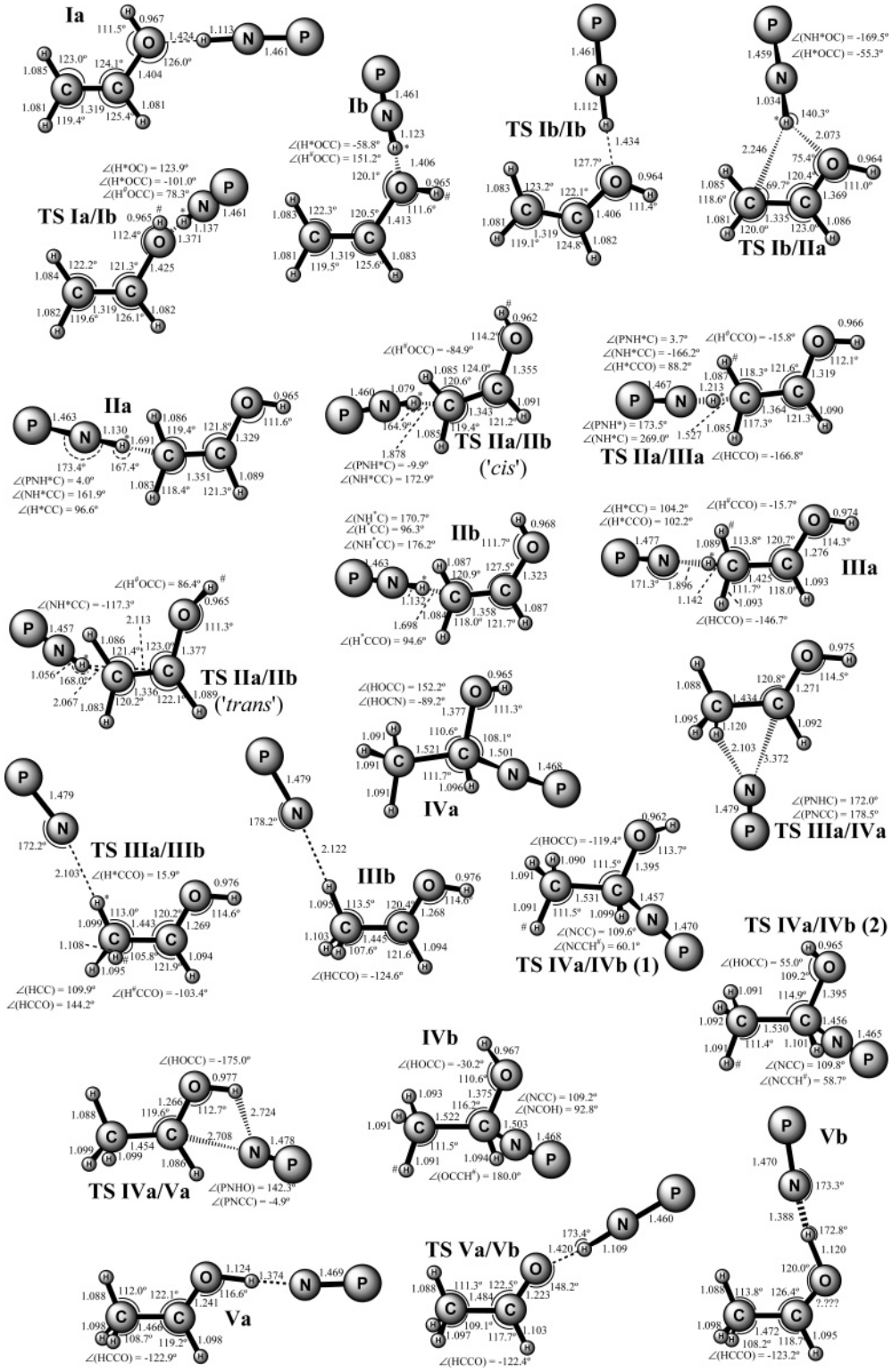

Figure 1. Geometries, optimized at the B3-LYP/CBSB7 level of theory, of $[C_2H_5NOP^+]$ stationary points relevant to the triple-play proton-transfer mechanism between $CH_2CHOH_2^+$ and PN. Bond lengths, in angstroms, and bond angles and dihedral angles, in degrees, are given for all species: when bond angles and dihedrals are not provided, this indicates near-linearity or near-planarity of the moiety in question. Minima **Ia**, **IIIb**, **Va**, and **Vb** and transition structures (TSs) **Ib**/**Ib** and **Va**/**Vb** possess C_s symmetry; all other stationary points shown are asymmetric.

transfer from O to N, subsequent migration of PNH^+, and proton transfer back to O.

As with **Va** and **Vb**, rotamers exist also for each of the minima **I**−**IV**. The barriers between pairs of rotamers are not large: in all instances, the relevant transition structure (TS) lies not more than 20 kJ mol^{-1} higher in energy than the higher-energy rotamer, which in turn is always within 10 kJ mol^{-1} of the lower-energy rotamer. Interconversion between rotamers, for example, **Ia** ↔ **Ib**, is therefore expected to be quite facile.[63] Several sections of the overall isomerization process are also attended by notably slight barriers: conversion from structure **IIa** → **IIIa** → **IVa** should therefore also be quite facile.

Not all of the minima involved in the proton-transfer triple play are true proton-bound dimers. The important structure **IVa** (as well as its rotamer **IVb**) is, in essence, a fully covalently bonded molecular ion involving a C−N bond which at 1.50 Å

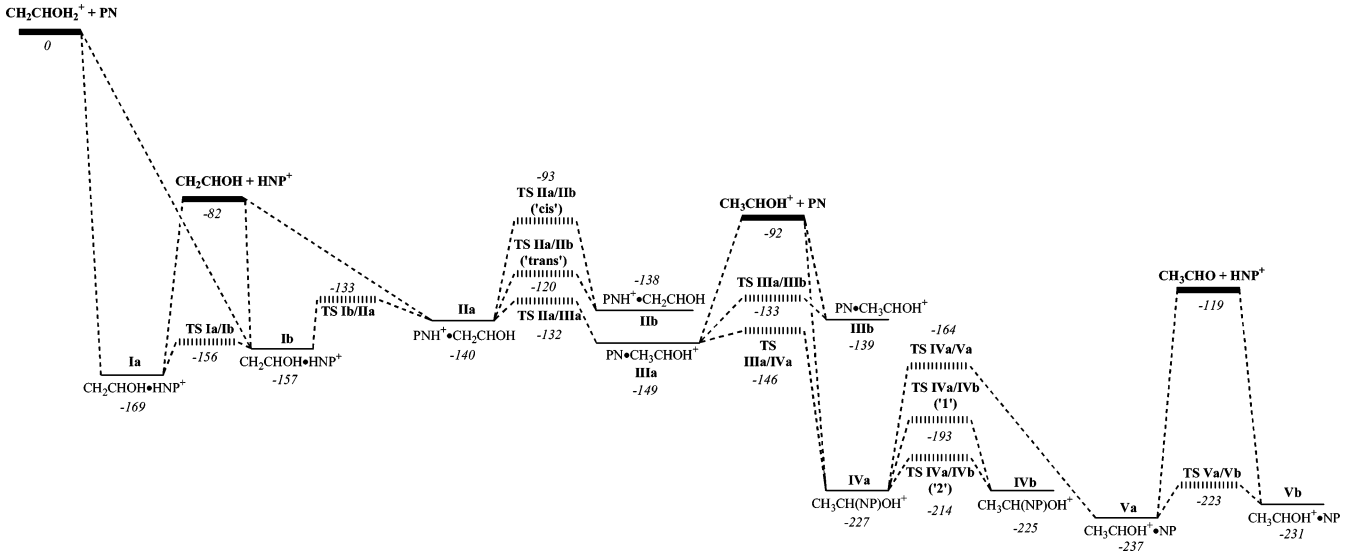

Figure 2. Schematic representation of the relationships between stationary points relevant to the triple-play mechanism on the $[C_2H_5NOP^+]$ potential energy surface. Local minima are denoted as solid lines, transition states (and connections between stationary points) as dashed lines, and bimolecular reactant or product combinations as bold lines. The CBS-QB3 values of the 298 K relative enthalpies, rounded to the nearest kilojoule per mole, are shown in italics.

is quite credible as a single bond between carbon and nitrogen. This species arises through migration of PN from the weak β-CH-coordinated CH_3CHOH^+/PN dimer **IIIa** and appears to subvert direct transfer of PN from the protonated β-carbon to the protonated oxygen of acetaldehyde. Numerous and rigorous efforts were made to locate a transition structure connecting **III** to **V**, bypassing the molecular ion **IV**: all such efforts were unsuccessful. The exothermic conversion of **IVa** to **Va**, by C−N bond cleavage and subsequent PN relocation, is energetically demanding from a local perspective—the relevant barrier is more than 60 kJ mol^{-1} higher in energy than structure **IVa**—but occurs on a portion of the potential energy surface which is overall quite deeply submerged, and should therefore be comparatively facile. The total energy difference between **IVa** and **Va** is quite slight: the molecular ion **IVa** lies only 13 kJ mol^{-1} above the proton-bound dimer **Va**. Nevertheless, the latter structure can more readily dissociate to bimolecular products: the lowest-energy product pair, $CH_3CHO + PNH^+$, is accessible from **Va** (or **Vb**) but not directly from **IVa** (or **IVb**).

Figure 2 provides a schematic overview of the topography of the CBS-QB3 potential energy surface, with regard to the interplay of proton transfer and tautomerization via the triple-play mechanism outlined above.

3.4. Other Stationary Points on the $[C_2H_5O/PN]^+$ Potential Energy Surface. Any 10-atom potential energy surface featuring five different atom types can be expected to contain a plethora of minima, and the $[C_2H_5NOP]^+$ surface fulfils this expectation. We have restricted our quest for further minima on this surface to those species which can arise from simple addition of neutral (or protonated) PN to protonated (or neutral) C_2H_4O. Accordingly, we have isolated an additional 16 minima **VI**−**XXI** (where the Roman numeric labels correspond to the ordering from lowest- to highest-energy isomer at the CBS-QB3 level of theory). These species are documented in Table 4 and depicted in Figure 3. It is highly probable that the identified minima are not exhaustive, but we contend that the quest undertaken to uncover these structures has likely captured all of the species which can arise without insertion of one or more heavy atoms into either the C−C, C−O, or P−N bond. Such insertion is expected to require the surmounting of significant activation energy barriers, suggesting that species not in Figure 1 or Figure 3 are reasonably remote prospects for formation via the reaction of $H_2CCHOH_2^+ + PN$. We have included, however, some structures involving PN insertion in C−O when the oxygen is nominally equivalent to an attached water ligand, as it is in $H_2CCHOH_2^+$ itself.

Of the "other" minima located, one species, *c*-(CH_2CH_2-OPNH) (**VI**), is particularly notable. This structure has by far the lowest total energy of any isolated here and lies over 110 kJ mol^{-1} below the lowest-energy isomer (**Va**) of those surveyed in section 3.3. For this reason, if structure **VI** is accessible from the reactants $CH_2CHOH_2^+ + PN$, it is likely to constitute an important sink as the thermochemically most favored adduct ion. However, there is no straighforward mechanism by which it appears feasible to produce **VI** from protonated vinyl alcohol. This low-energy molecular ion is a more likely product of the reaction between protonated ethylene oxide, *c*-$C_2H_4OH^+$, and PN.

Another two structures, **VII** and **XI**, also warrant consideration as feasible intermediates in the reaction of $CH_2CHOH_2^+ + PN$. Both are comparatively low in total energy (E_{rel} = −227.6 and −169.6 kJ mol^{-1}, relative to reactants) and show close structural relationships with neutral or protonated vinyl alcohol. The structure **VII** can in principle arise through PN insertion into the C−O bond of the reactant $CH_2CHOH_2^+$, while **XI** is a possible product of PNH^+ migration from isomer **Ib**. Furthermore, **VII** can dissociate to give the bimolecular product combination $H_2CCHNP^+ + H_2O$ (see Table 4) whose formation from $CH_2CHOH_2^+ + PN$ is substantially more exothermic than the lowest-energy proton-transfer product pair $CH_3CHO + PNH^+$. However, the transition state located for PN insertion (TS **VII**) is considerably (∼60 kJ mol^{-1}) higher in total energy than the separated reactants, suggesting that **VII** is not an accessible intermediate from $CH_2CHOH_2^+ + PN$. In contrast, the transition state **I**/**XI** implicated in the formation of **XI** is clearly accessible and represents a viable alternative to the production from **Ib** of the "proton-bound dimer" **IIa**. Direct interconversion between **IIa** and **XI** appears not to be viable, since no interconnecting transition structure was found between these minima. The possible formation of **XI** likely has a minor impact on the course of the overall reaction: rearrangement to **IIa** is still feasible via reversion to **Ib**, while dissociation of **XI**

TABLE 4: CBS-QB3 Total Energies of Other Local Minima Located on the $[C_2H_5O/PN]^+$ Potential Energy Surface

structure	ZPE[a]/mhartrees	E_0 (0 K)[b]/hartrees	H_0 (298 K)[c]/hartrees	E_{rel} (0 K)[d]/kJ mol^{-1}	ΔH_{rel} (298 K)[d]/kJ mol^{-1}
c-$(CH_2CH_2OPNH)^+$ (**VI**)	78.044	−549.538 696	−549.532 832	−351.1	−357.9
$H_2CCHNP^+ \cdot OH_2$ (**VII**)	71.421	−549.491 647	−549.482 844	−227.6	−226.7
$PNCH_2CH_2OH^+$ (**VIII**)	75.791	−549.487 884	−549.480 979	−217.7	−221.8
c-$(CH_2CH_2OHPN)^+$ (**IX**)	76.408	−549.481 949	−549.475 550	−202.1	−207.5
c-$(CH_2CH_2OP)NH^+$ (**X**)	74.612	−549.480 494	−549.474 206	−198.3	−204.0
$HNPCH_2CHOH^+$ (**XI**)	73.233	−549.469 584	−549.462 227	−169.6	−172.5
TS **I**/**XI**[e]	71.227	−549.454 087	−549.447 014	−129.0	−132.6
c-$(CH_2CH_2OPHN)^+$ (**XII**)	73.970	−549.452 912	−549.446 898	−125.9	−132.3
c-$(CH_2CH_2ONHP)^+$ (**XIII**)	76.922	−549.448 310	−549.442 630	−113.8	−121.1
$CH_3CH_2ONP^+$ (**XIV**)	74.574	−549.420 373	−549.413 308	−40.4	−44.1
c-$(CH_2CH_2OHNP)^+$ (**XV**)	75.382	−549.406 200	−549.400 171	−3.2	−9.6
c-$(CH_2CH_2ON)PH^+$ (**XVI**)	74.228	−549.404 830	−549.398 830	0.4	−6.1
$CH_2CHOH_2 \cdot PN^+$ (**XVII**)	70.866	−549.399 457	−549.390 316	14.5	16.3
c-$(CH_2CH_2ONPH)^+$ (**XVIII**)	72.840	−549.392 594	−549.386 673	32.5	25.8
$H_2CCHPNOH_2^+$ (**XIX**)	72.182	−549.384 862	−549.377 149	52.8	50.8
TS **VII**[e]	68.881	−549.381 680	−549.373 672	61.1	60.0
$CH_3CH_2OPN^+$ (**XX**)	71.635	−549.380 595	−549.372471	64.01	63.
$CH_2CHOHN(H)P^+$ (**XXI**)	68.299	−549.361 286	−549.353 083	114.7	114.0
$H_2CCHNP^+ + H_2O$	68.719	−549.470 138	−549.461 071	−171.1	−169.5
$H_2CCHPN^+ + H_2O$	65.600	−549.360 132	−549.350 109	117.7	121.8

[a] Zero-point vibrational energy in millihartrees (1 mhartree = 2.6255 kJ mol^{-1}), calculated at the B3-LYP/6-311G(2d,d,p) level of theory. [b] Calculated total energy including zero-point vibrational energy. [c] Calculated enthalpy including zero-point vibrational energy and thermal corrections. [d] Calculated total energy (E_0), or enthalpy (H_0), at the indicated temperature, expressed relative to the reactants $CH_2CHOH_2^+ + PN$. [e] Has one imaginary vibrational frequency at the B3-LYP/6-311G(2d,d,p) level of theory.

can lead only to $CH_2CHOH + PNH^+$, the same product pair which is directly accessible from the precursor intermediate **Ib**. The barrier heights for the formation of **IIa** and **XI** are closely comparable, and detailed kinetic modeling would be needed to evaluate the influence of **XI** as a possible obstacle to the ultimate formation of $CH_3CHO + PNH^+$ via intermediate **IIa** and the subsequent minima.

Other intermediates in Figure 3 are unlikely to feature significantly in the reaction of $H_2CCHOH_2^+ + PN$, on thermochemical or kinetic grounds. The formation of structures **XVII**−**XXI** is endothermic, while the other lower-energy isomers would all require the occurrence (at least) of 1,2-hydrogen shifts which are expected to be inhibited by significant barriers. Several of these structures may, however, be accessible through the reaction of protonated ethylene oxide, *c*-$C_2H_5O^+$, with PN.

3.5. General Discussion. The reaction of $CH_2CHOH_2^+$ with PN holds some relevance for interstellar cloud chemical evolution, since PN, CH_2CHOH, and CH_3CHO are all known constituents of various interstellar clouds. This reaction also appears to feature an interesting extension of the general proton-transport catalysis mechanism, as discussed above. It is also possible to view the mechanism from an alternative perspective, that of an acid-catalyzed keto/enol tautomerization (although CH_3CHO is not strictly a ketone). In this context, we note that there are several precedents for the occurrence of keto/enol tautomerization in ion/molecule chemistry.[64−67] However, these previous studies have reported the occurrence of fragmentation of metal ion adducts of ketones[64,65] or of base-catalyzed[66,67] isomerization of ionized acetone. There do not appear to be any previous studies of an acid-catalyzed keto/enol tautomerization, and for this reason, the reaction of $CH_2CHOH_2^+$ with PN (or with another appropriate molecule with a proton affinity between PA($CH_3CH\boldsymbol{O}$) and PA($\boldsymbol{C}H_2CHOH$), such as those in Table 2) may be of considerable interest as a fundamental example of a generic organic chemistry process.[68]

The reaction of $CH_2CHOH_2^+$ with PN can also serve as a useful prototype for proton-transfer effected tautomerization in general. There are, in principle, four broad classes of proton-transfer reactivity exhibited by $CH_2CHOH_2^+$ with various neutrals X, as a function of the reactant neutral proton affinity PA(X):

(a) $PA(X) < PA(CH_2CH\boldsymbol{O}H)$

(b) $PA(CH_2CH\boldsymbol{O}H) < PA(X) < PA(CH_3CH\boldsymbol{O})$

(c) $PA(CH_3CH\boldsymbol{O}) < PA(X) < PA(\boldsymbol{C}H_2CHOH)$

(d) $PA(\boldsymbol{C}H_2CHOH) < PA(X)$

Here, the literature values[3] of the threshold proton affinities separating these classes are 721.7, 768.5, and 811.2 kJ mol^{-1}, respectively. The proton-transfer thermochemistry dictates that, for neutrals X fitting case a, proton transfer from $CH_2CHOH_2^+$ is endothermic. Such reactions are likely to be dominated by association or by bimolecular reactions involving rearrangement other than proton transfer. At the opposite end, when a neutral X conforms to case d, straightforward proton transfer to produce $XH^+ + CH_2CHOH$ is highly exothermic and is expected to dominate (depending on the efficiency of competing association and other rearrangement channels); a second intracomplex proton-transfer step, to produce $CH_3CHOH^+ + X$, is thermochemically disadvantaged. This second proton-transfer step is viable for cases b and c, which differ in that case c also energetically favors the subsequent proton transfer from CH_3CHOH^+ to X but case b does not. While the precise threshold PA values listed above obviously apply only to the protonated CH_2CHOH/CH_3CHO system, the division of proton-transfer chemistry into four cases can be generalized to all systems where a higher-energy tautomer has two accessible protonated forms, one of which corresponds also to the protonated form of a lower-energy tautomer. Such structural and energetic considerations are likely to be frequently encountered among ketones, aldehydes (and their thio- counterparts), nitriles, and imines.

Experimental study of the $CH_2CHOH_2^+ + PN$ reaction is likely to be impeded by several factors. First, the reactant ion $CH_2CHOH_2^+$ is difficult to generate in pure form, due to the instability of the parent neutral vinyl alcohol. A SIFT study[24] has indicated that $CH_2CHOH_2^+$ is produced in moderate yield through the termolecular association of $H_3O^+ + C_2H_2$, but this reaction also generates $C_2H_5O^+$ in another isomeric form, probably the electrostatic adduct $H_3O^+ \cdot C_2H_2$. Second, the reactant neutral PN is unstable under conventional laboratory conditions. Third, elucidation of the product channels requires

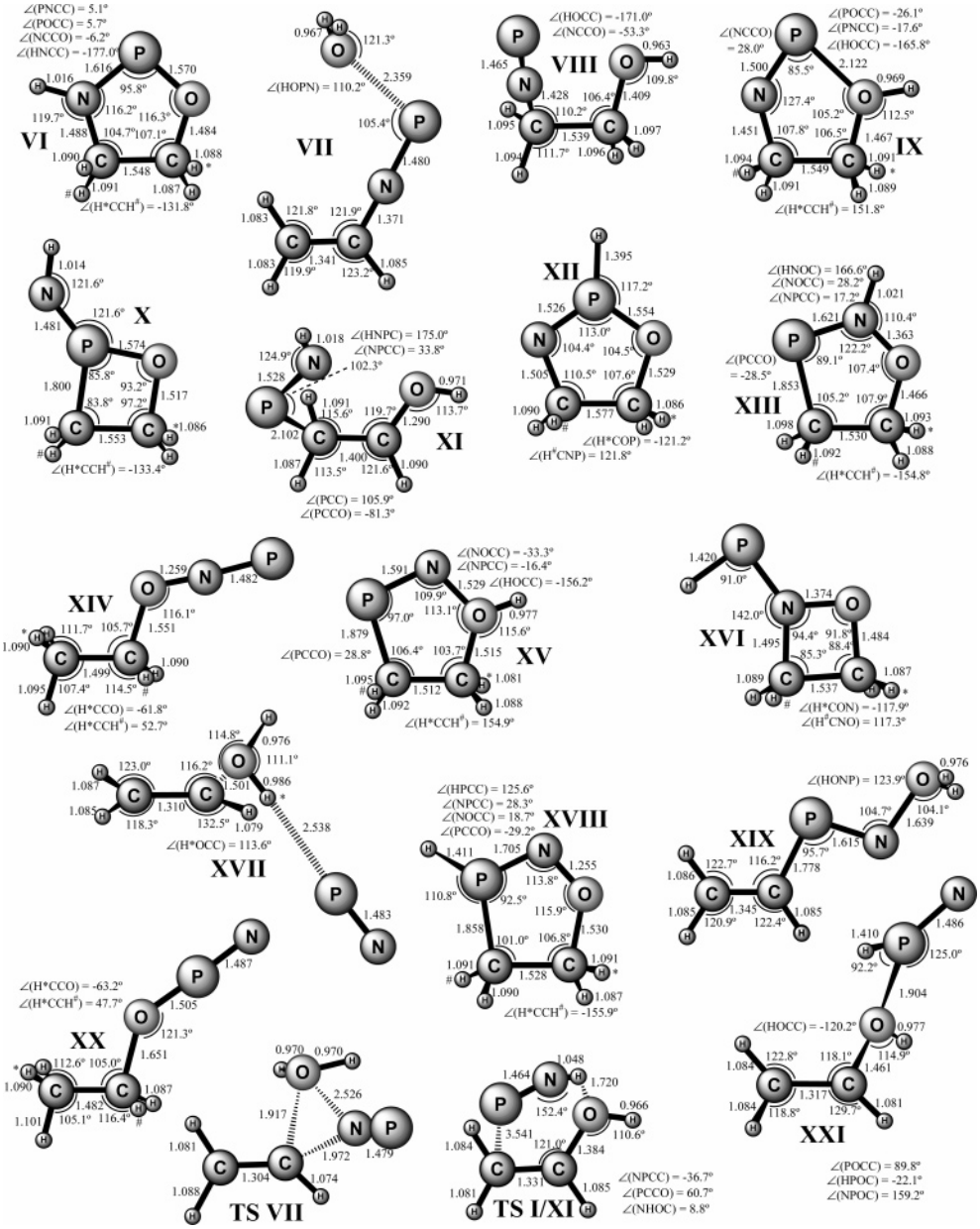

Figure 3. Geometries, optimized at the B3-LYP/CBSB7 level of theory, of various additional [$C_2H_5NOP^+$] minima located in the present work. Bond lengths are given in angstroms, and bond angles and dihedral angles are in degrees. Structures **VII**, **X**, **XII**, **XIV**, **XVI**, **XIX**, and **XX** possess C_s symmetry; all other stationary points shown are asymmetric.

a method of distinguishing the isomeric prospective products CH_2CHOH and CH_3CHO, which would seem to necessitate spectroscopic identification of an extremely low concentration of either of these products, since typically the number density of the parent ion $C_2H_5O^+$ would not exceed $\sim 10^9$ cm^{-3} in a selected-ion flow tube or other multicollision ion/molecule reactor. While mass-spectrometric techniques for distinguishing isomeric ions at such low concentrations are reasonably well-established,[69] such a sensitive diagnostic for neutral products would appear elusive.

4. Conclusions

Quantum chemical calculations show that a viable, fully submerged minimum-energy pathway exists for the proton-transport catalysis process converting $CH_2CHOH_2^+$ + PN to CH_3CHO + PNH^+, a mechanism which we describe as a proton-transfer triple play. This process, for which laboratory verification is expected to be problematic, is of interest not only in the context of interstellar chemical evolution but also as a gas-phase analogue of the condensed-phase mechanism of acid-catalyzed keto/enol tautomerization. While competing product channels exist, there are no apparent accessible bimolecular product channels of greater exothermicity, suggesting that competition from these other channels should be minimal.

Acknowledgment. This work used the supercomputing resources of the Australian Partnership of Advanced Computing.

References and Notes

(1) In baseball, a "triple play" can be considered as the interception of three bases (proton acceptors?) before the completion of a play.

(2) Lias, S. G.; Liebman, J. F.; Levin, R. D. *J. Phys. Chem. Ref. Data* **1984**, *13*, 695.

(3) Hunter, E. P. L.; Lias, S. G. *J. Phys. Chem. Ref. Data* **1998**, *27*, 413.

(4) Roche, A. E.; Sutton, M. M.; Bohme, D. K.; Schiff, H. I. *J. Chem. Phys.* **1971**, *55*, 5480.

(5) Dixon, D. A.; Komornocki, A.; Kramer, W. P. *J. Chem. Phys.* **1984**, *81*, 3603.
(6) Freeman, C. G.; Knight, J. S.; Love, J. G.; McEwan, M. J. *Int. J. Mass Spectrom. Ion Processes* **1987**, *80*, 255.
(7) Bohme, D. K. *Int. J. Mass Spectrom Ion Processes* **1992**, *115*, 95.
(8) Petrie, S.; Freeman, C. G.; Meotner, M.; Ferguson, E. E.; McEwan, M. J. *J. Am. Chem. Soc.* **1990**, *112*, 7121.
(9) Jones, T. T. C.; Raouf, A. S. M.; Birkinshaw, K.; Twiddy, N. D. *J. Phys. B: At. Mol. Opt. Phys.* **1981**, *14*, 2713.
(10) Ferguson, E. E. *Chem. Phys. Lett.* **1989**, *156*, 319.
(11) Fox, A.; Bohme, D. K. *Chem. Phys. Lett.* **1991**, *187*, 541.
(12) Chyall, L. J.; Squires, R. R. *J. Phys. Chem.* **1996**, *100*, 16435.
(13) Gauld, J. W.; Audier, H.; Fossey, J.; Radom, L. *J. Am. Chem. Soc.* **1996**, *118*, 6299.
(14) van der Rest, G.; Nedev, H.; Chamot-Rooke, J.; Mourgues, P.; McMahon, T. B.; Audier, H. E. *Int. J. Mass Spectrom.* **2000**, *202*, 161.
(15) Trikoupis, M. A.; Burgers, P. C.; Ruttink, P. J. A.; Terlouw, J. K. *Int. J. Mass Spectrom.* **2001**, *210*, 489.
(16) Wong, C. Y.; Ruttink, P. J. A.; Burgers, P. C.; Terlouw, J. K. *Chem. Phys. Lett.* **2004**, *390*, 176.
(17) Wong, C. Y.; Ruttink, P. J. A.; Burgers, P. C.; Terlouw, J. K. *Chem. Phys. Lett.* **2004**, *387*, 204.
(18) DeFrees, D. J.; McLean, A. D.; Herbst, E. *Astrophys. J.* **1984**, *279*, 322.
(19) Ziurys, L. M.; Apponi, A. J. *Astrophys. J.* **1995**, *455*, L73.
(20) Herbst, E.; Woon, D. E. *Astrophys. J.* **1996**, *463*, L113.
(21) Ikeda, M.; Ohishi, M.; Nummelin, A.; Dickens, J. E.; Bergman, P.; Hjalmarson, A.; Irvine, W. M. *Astrophys. J.* **2001**, *560*, 792.
(22) Turner, B. E.; Apponi, A. J. *Astrophys. J.* **2001**, *561*, L207.
(23) Herbst, E. *Astrophys. J.* **1987**, *313*, 867.
(24) Fairley, D. A.; Scott, G. B. I.; Freeman, C. G.; Maclagan, R. G. A. R.; McEwan, M J. *J. Chem. Soc., Faraday Trans.* **1996**, *92*, 1305.
(25) Beauchamp, J. L.; Dunbar, R. C. *J. Am. Chem. Soc.* **1970**, *92*, 1477.
(26) Solka, B. H.; Russell, M. E. *J. Phys. Chem.* **1974**, *78*, 1268.
(27) Bowen, R. D.; Williams, D. H.; Hvistendahl, G. *J. Am. Chem. Soc.* **1977**, *99*, 7509.
(28) Lossing, F. P. *J. Am. Chem. Soc.* **1977**, *99*, 7526.
(29) Lischka, H.; Koehler, H. J. *Chem. Phys. Lett.* **1979**, *63*, 326.
(30) Nobes, R. H.; Rodwell, W. R.; Bouma, W. J.; Radom, L. *J. Am. Chem. Soc.* **1981**, *103*, 1913.
(31) Nguyen, M. T.; Hegarty, A. F.; Ha, T. K.; De Mare, G. R. *J. Chem. Soc., Perkin Trans. 2* **1986**, 147.
(32) Bock, C. W.; George, P.; Glusker, J. P. *J. Org. Chem.* **1993**, *58*, 5816.
(33) Curtiss, L. A.; Lucas, D. J.; Pople, J. A. *J. Chem. Phys.* **1995**, *102*, 3292.
(34) O'Hair, R. A. J.; Freitas, M. A.; Gronert, S.; Schmidt, J. A. R.; Williams, T. D. *J. Org. Chem.* **1995**, *60*, 1990.
(35) Hudson, C. E.; McAdoo, D. J. *Int. J. Mass Spectrom.* **2004**, *232*, 17.
(36) Turner, B. E.; Bally, J. *Astrophys. J.* **1987**, *321*, L75.
(37) Ziurys, L. M. *Astrophys. J.* **1987**, *321*, L81.
(38) East, A. L. L.; Smith, B. J.; Radom, L. *J. Am. Chem. Soc.* **1997**, *119*, 9014.
(39) Hammerum, S. *Int. J. Mass Spectrom.* **1997**, *165*, 63.
(40) Hammerum, S. *Chem. Phys. Lett.* **1999**, *300*, 529.
(41) Ochterski, J. W.; Petersson, G. A.; Montgomery, J. A., Jr. *J. Chem. Phys.* **1996**, *104*, 2598.
(42) Montgomery, J. A., Jr.; Frisch, M. J.; Ochterski, J. W.; Petersson, G. A. *J. Chem. Phys.* **1999**, *110*, 2822.
(43) Montgomery, J. A., Jr.; Ochterski, J. W.; Petersson, G. A. *J. Chem. Phys.* **1994**, *101*, 5900.
(44) Unravelling the acronym "CBS-QB3" is nontrivial. "CBS" stands for the "complete basis set" approach, and "B3" is a grammatical contraction of "B3-LYP", a hybrid density functional method combining Becke's three-parameter exchange functional[45] with the correlation functional of Lee, Yang, and Parr.[46] The latter method is employed in CBS-QB3,[42] using the 6-311G(2d,2p) basis set[42] to yield optimized geometries and zero-point vibrational energies. The "Q" in "CBS-QB3" denotes the implementation of quadratic configuration interaction including single, double, and perturbative triple excitations, QCISD(T), as the most rigorous treatment of electron correlation employed in the earlier CBS-Q method,[41] although ironically CBS-QB3[42] *does not* itself feature QCISD(T) in any computational steps, favoring instead the CCSD(T)—or coupled-cluster with single, double, and perturbative triple excitations[47,48]—level of theory.
(45) Becke, A. D. *J. Chem. Phys.* **1993**, *98*, 5648.
(46) Lee, C.; Yang, W.; Parr, R. G. *Phys. Rev. B* **1988**, *37*, 785.
(47) Cizek, J. *Adv. Chem. Phys.* **1969**, *14*, 35.
(48) Pople, J. A.; Head-Gordon, M.; Raghavachari, K. *J. Chem. Phys.* **1987**, *87*, 5968.
(49) Dunning, T. H., Jr. *J. Chem. Phys.* **1989**, *90*, 1007.
(50) Kendall, R. A.; Dunning, T. H., Jr.; Harrison, R. J. *J. Chem. Phys.* **1992**, *96*, 6796.
(51) Woon, D. E.; Dunning, T. H., Jr. *J. Chem. Phys.* **1993**, *98*, 1358.
(52) Frisch, M. J.; et al. *Gaussian 98*, rev. A.7; Gaussian Inc.: Pittsburgh, PA, 1998.
(53) Smith, B. J.; Radom, L. *J. Am. Chem. Soc.* **1993**, *115*, 4885.
(54) Lias, S. G.; Bartmess, J. E.; Liebman, J. F.; Holmes, J. L.; Levin, R. D.; Mallard, W. G. *J. Phys. Chem. Ref. Data* **1988**, *17* (Suppl. 1).
(55) Fox, A.; Wlodek, S.; Hopkinson, A. C.; Lien, M. H.; Sylvain, M.; Rodriquez, C.; Bohme, D. K. *J. Phys. Chem.* **1989**, *93*, 1549.
(56) Botschwina, P.; Rosmus, P. *J. Chem. Phys.* **1985**, *82*, 1420.
(57) Lucas, D. L.; Curtiss, L. A.; Pople, J. A. *J. Chem. Phys.* **1993**, *99*, 6697.
(58) Rodriquez, C. F.; Cunje, A.; Hopkinson, A. C. *THEOCHEM* **1998**, *430*, 149.
(59) Adams, N. G.; McIntosh, B. J. *Astron. Astrophys.* **1990**, *232*, 443.
(60) Our calculated PN dipole moment of $\mu_D = 2.825$ D (at the B3-LYP/CBSB7 level of theory) or 2.870 D (B3-LYP/aug-cc-pVTZ) agrees very well, in both instances, with the experimental value 2.746 D[61] as well as with a previous theoretical determination of 2.891 D.[62]
(61) Raymonda, J. W.; Klemperer, W. A. *J. Chem. Phys.* **1971**, *55*, 232.
(62) Peterson, K. A.; Woods, R. C. *J. Chem. Phys.* **1990**, *92*, 6061.
(63) Note that a minor inconsistency is evident in the relative energies of the minimum **Ib** and its C_s-symmetric transition state to inversion, **TS Ib**/**Ib**. At the B3-LYP/CBSB7 level of theory, **Ib** lies 1.4 kJ mol^{-1} *lower* in energy than its identified transition state, but when the composite CBS-QB3 energies are evaluated, **Ib** is 7.7 kJ mol^{-1} *higher* in energy than the putative saddle point. This discrepancy is presumed to arise because of differences in the potential energy surface topography between the B3-LYP/CBSB7 and "full CBS-QB3" levels of theory, and further calculations may be necessary to satisfactorily resolve the structure of **Ib**.
(64) Zagorevskii, D. V.; Volkova, T. B.; Yakushin, S. O.; Antipov, B. G.; Nekrasov, Yu. S. *Org. Mass Spectrom.* **1991**, *26*, 748.
(65) Hall, B. J.; Brodbelt, J. S. *J. Am. Soc. Mass Spectrom.* **1999**, *10*, 402.
(66) Mourgues, P.; Chamot-Rooke, J.; van der Rest, G.; Nedev, H.; Audier, H. E.; McMahon, T. B. *Int. J. Mass Spectrom.* **2001**, *210/211*, 429.
(67) Mourgues, P.; Chamot-Rooke, J.; van der Rest, G.; Audier, H. E.; McMahon, T. B. *Adv. Mass Spectrom.* **2001**, *15*, 723.
(68) Note, also, that "ketone" CH_3CHO and enol CH_2CHOH obey the general tendency for condensed-phase ketones to display greater stability than their enolic counterparts, whereas this is not true of the other system to have received detailed study:[66,67] the radical ion $CH_3COCH_3^{+\bullet}$ is less stable than its enol isomer $CH_3C(OH)CH_2^{+\bullet}$.[66]
(69) McEwan, M. J. *Adv. Gas Phase Ion Chem.* **1992**, *1*, 1.